

Primordial Black Holes from Supersymmetry in the Early Universe

Eric Cotner¹ and Alexander Kusenko^{1,2}

¹*Department of Physics and Astronomy, University of California, Los Angeles Los Angeles, California 90095-1547, USA*

²*Kavli Institute for the Physics and Mathematics of the Universe (WPI), UTIAS The University of Tokyo, Kashiwa, Chiba 277-8583, Japan*

(Received 12 December 2016; revised manuscript received 30 March 2017; published 21 July 2017)

Supersymmetric extensions of the standard model generically predict that in the early Universe a scalar condensate can form and fragment into Q balls before decaying. If the Q balls dominate the energy density for some period of time, the relatively large fluctuations in their number density can lead to formation of primordial black holes (PBH). Other scalar fields, unrelated to supersymmetry, can play a similar role. For a general charged scalar field, this robust mechanism can generate black holes over the entire mass range allowed by observational constraints, with a sufficient abundance to account for all dark matter in some parameter ranges. In the case of supersymmetry the mass range is limited from above by 10^{23} g. We also comment on the role that topological defects can play for PBH formation in a similar fashion.

DOI: 10.1103/PhysRevLett.119.031103

It is a long-standing question whether black holes could form in the early Universe [1–12]. Primordial black holes (PBH) could account for all or part of dark matter [1–6,8–12], they could be responsible for some of the gravitational wave signals observed by LIGO [13–15], and they could provide seeds for supermassive black holes [7]. A number of scenarios for black hole formation have been considered [5], and many of them rely on a spectrum of primordial density perturbations that has some extra power on certain length scales, which can be accomplished by means of tuning an inflaton potential.

In this Letter we present a more generic scenario for PBH formation in the early Universe, which does not rely on any particular spectrum of density perturbations from inflation. Scalar fields with slowly growing potentials form a coherent condensate at the end of inflation [16–19]. In general, the condensate is not stable, and it breaks up in lumps, which evolve into Q balls [20]. The gas of Q balls contains a relatively low number of lumps per horizon, and the mass contained in these lumps fluctuates significantly from place to place. This creates relatively large fluctuations of mass density in Q balls across both subhorizon and superhorizon distances. Since the energy density of a gas of Q balls redshifts as mass, it can come to dominate the energy density temporarily, until the Q balls decay, returning the Universe to a radiation dominated era. The growth of structure during the Q -ball dominated phase can lead to copious production of primordial black holes.

Formation of Q balls requires nothing more than some scalar field with a relatively flat potential at the end of inflation. For example, supersymmetric theories predict the existence of scalar fields with flat potentials. PBH formation in supersymmetric theories is, therefore, likely, even if the scale of supersymmetry breaking exceeds the reach of existing colliders.

A similar process can occur with topological defects, which can also lead to relatively large inhomogeneities. The discussion of topological defects is complicated by their nontrivial evolution. We focus primarily on Q balls, and briefly comment on topological defects below.

Formation of Q balls occurs by fragmentation of a scalar condensate after inflation [20]. While supersymmetry is a well-motivated theory for scalar fields carrying global charges and having flat potentials [18,21], our discussion can be easily generalized to an arbitrary scalar field with a global $U(1)$ symmetry in the potential. Supersymmetric potentials generically contain flat directions that are lifted only by supersymmetry breaking terms. Some of the scalar fields that parametrize the flat directions carry a conserved $U(1)$ quantum number, such as the baryon or lepton number. During inflation, these fields develop a large vacuum expectation value [16–19], leading to a large, nonzero global charge density. When inflation is over, the scalar condensate $\phi(t) = \phi_0(t) \exp\{i\theta(t)\}$ relaxes to the minimum of the potential by a coherent classical motion with $\dot{\theta} \neq 0$ due to the initial conditions and possible CP violation at a high scale.

The initially homogeneous condensate is unstable with respect to fragmentation into nontopological solitons, Q balls [22]. Q balls exist in the spectrum of every supersymmetric generalization of the standard model [23,24], and they can be stable or long-lived along a flat direction [20,25]. In the case of a relatively large charge density (which is necessary for Affleck-Dine baryogenesis [18,21]), the stability of Q balls can be analyzed analytically [20,26,27]; these results agree well with numerical simulations [28]. One finds that the almost homogeneous condensate develops an instability with wave numbers in the range $0 < k < k_{\max}$, where $k_{\max} = \sqrt{\omega^2 - V''(\phi_0)}$, and $\omega = \dot{\theta}$. The fastest growing modes of instability have a

wavelength $\sim 10^{-2\pm 1}$ of the horizon size at the time of fragmentation, and they create isolated lumps of condensate that evolve into Q balls. Numerical simulations [28,29] indicate that most of the condensate ends up in lumps. However, since the mass of Q balls is a nonlinear function of the Q -ball size, Q -ball formation, in general, leads to a nonuniform distribution of energy density in the matter component represented by the scalar condensate. Q balls can also form when the charge density is small or 0, in which case both positively and negatively charged Q balls are produced [28]; here we do not consider this possibility.

If the potential is flat, a Q ball with global charge Q has mass $M \propto |Q|^{3/4}$ [20,25]. The density fluctuations arise from the nonlinear relation between M and Q . In general, $M \sim |Q|^\alpha$, where α depends on the potential. If $\alpha = 1$, some density fluctuations may arise from global charge redistribution during fragmentation. We do not consider this possibility here, and we limit our discussion to $\alpha = 3/4$.

Q-ball number distribution.—Let us consider N identical Q balls in some volume V at the time of fragmentation t_f . We assume that the probability to find N Q balls in a given volume V follows a Poisson distribution,

$$p(N, V) = e^{-(N_f V/V_f)} \frac{(N_f V/V_f)^N}{N!}, \quad N \in \mathbb{Z}^+, \quad (1)$$

where N_f is the average number of Q balls per horizon (within volume $V_f = (4\pi/3)t_f^3$, the horizon volume at fragmentation). The mass of a volume containing N Q balls is given by $M(N) = NM_{Q\text{ball}} = \Lambda N Q^\alpha$. If this mass is large enough, it becomes the mass of the black hole resulting from the collapse. The charge within the volume V at fragmentation is assumed to be distributed equally among the N Q balls, so that $NQ = Q_f V/V_f$ (with Q_f being the total charge on the horizon at t_f), which gives us the Q -ball cluster distribution function F_Q ,

$$F_Q(M, N, V) = \delta\left(M - M_f \left(\frac{N}{N_f}\right)^{1-\alpha} \left(\frac{V}{V_f}\right)^\alpha\right) p(N, V), \quad (2)$$

where $M_f = \Lambda Q_f^\alpha N_f^{1-\alpha}$ is the average Q -ball horizon mass at t_f . F_Q represents the probability density to find a mass M composed of N Q balls within a volume V .

The average background energy density (over the largest scales) in Q balls at t_f is then given by

$$\langle \rho_Q(t_f) \rangle = \lim_{V \rightarrow \infty} \frac{\langle M \rangle}{V} = \frac{M_f}{V_f}, \quad (3)$$

with the average performed over M and N .

Q balls are stable with respect to decay into scalar particles, but they can decay into fermions lighter than ω [30–32]. Q balls can also decay if the $U(1)$ symmetry is

broken by some higher-dimension operators [33–36]. We parametrize this decay by the total decay width $\Gamma_Q = 1/\tau_Q$, which includes all decay channels. The energy density in the form of Q balls scales with expansion of the Universe as decaying matter [37], and the decays also contribute to radiation density. We take this into account in a consistent manner using the analysis of Scherrer and Turner [37]. The energy density of Q balls then evolves as $\langle \rho_Q(t) \rangle = \langle \rho_Q(t_f) \rangle (a_f/a)^3 e^{(t_f-t)/\tau_Q}$, and we assume that at some time t_Q the Q balls come to dominate, as shown in Fig. 1.

Density perturbations can grow starting at time t_Q when the Universe becomes matter dominated [i.e., $\rho_R(t_Q) = \langle \rho_Q(t_Q) \rangle$] until the time when the Q balls decay, returning the Universe to a radiation dominated phase. The structures can grow on all length scales above some minimum size V_{\min} , which we take to be the volume containing an average number of Q balls $N_{\min} \sim 10$. This acts as a cutoff to the low-mass part of the PBH spectrum, but does not influence any larger scales, and we have checked that the results are not sensitive to this choice as long as $N_{\min} \ll N_f$.

The density contrast in Q balls at fragmentation $\delta(t_f)$ of a specific mass scale M composed of N Q balls within a volume V at t_f is given by

$$\delta(t_f) = \frac{\delta\rho}{\langle \rho_Q \rangle} = \frac{M/V}{\langle \rho_Q \rangle} - 1 = \left(\frac{N/N_f}{M/M_f}\right)^{\frac{1-\alpha}{\alpha}} - 1, \quad (4)$$

where in the last line we have used the argument of the delta function in Eq. (2) to eliminate V . Note that when $\alpha = 1$, the density perturbations vanish identically.

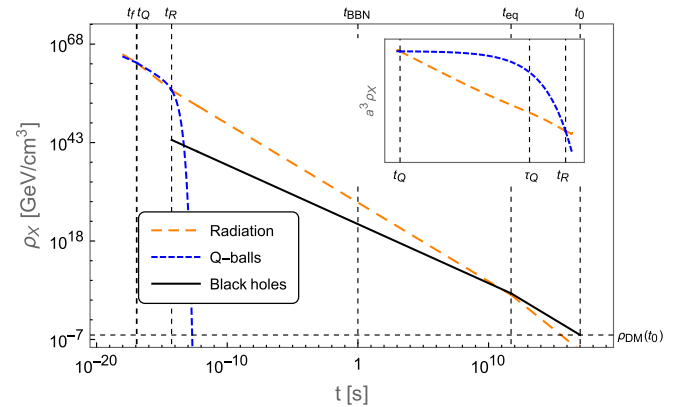


FIG. 1. Cosmological timeline corresponding to the production of PBH. The orange dashed line denotes radiation density ρ_R , the blue dashed line is Q -ball energy density $\langle \rho_Q \rangle$, and the black solid line is black hole density $\langle \rho_{\text{BH}} \rangle$. The inset in the upper right is a zoomed-in view of the early matter dominated era ($t_Q < t < t_R$), with density scaled by a^3 (so that nondecaying matter is represented by a straight horizontal line). The horizontal dashed line indicates the observed present-day dark matter density. Here the parameters correspond to the solid line in Fig. 3.

The density perturbations are frozen during the radiation dominated era, but they grow linearly in the scale factor during the Q -ball dominated epoch, $\delta(t) = \delta(t_f)(a/a_Q) = \delta(t_f)(t/t_Q)^{2/3}$. The structure growth generally goes nonlinear and decouples from the expansion around $\delta > \delta_c \sim 1.7$, at which point the overdense regions collapse and become gravitationally bound. However, some structures with $\delta < \delta_c$ can still collapse, and not all structures with $\delta > \delta_c$ are guaranteed to collapse into black holes. Because of nonsphericity of the gravitationally bound structures, only a fraction $\beta = \gamma\delta^{13/2}(t_R)(M/M_Q)^{13/3}$ [where $\gamma \approx 2 \times 10^{-2}$ and $M_Q = M_f(t_Q/t_f)^{3/2}$ is the horizon mass at the beginning of the Q -ball dominated era] actually collapses spherically to form black holes [9,38,39] by the end of the Q -ball dominated era (t_R). Structures with $\delta \geq \delta_c$ do not continue to grow (as perturbations are gravitationally bound at this point and cease developing), so that $\beta = \gamma\delta_c^{13/2}(M/M_Q)^{13/3}$ for $\delta(t_R) > \delta_c$. Despite these refinements, the outcome does not appear to depend sensitively on the value of δ_c .

Additional care must be taken to extend this to scales that enter the horizon during the Q -ball dominated era, and thus are not subject to the same amount of growth as the subhorizon modes. This can be done by calculating the time t_h at which a comoving superhorizon volume V at t_f reenters the horizon: $(a(t_h)/a_f)^3 V = V_h = (4\pi/3)t_h^3$. Then, the amplification of these superhorizon modes at the end of the Q -ball dominated era is given by $\delta(t_f)(a_R/a(t_h))$ rather than $\delta(t_f)(a_R/a(t_Q))$. Also, because this expression is only valid for small δ , we cap its value at $\beta_{\max} = 1$ to avoid collapse probabilities over unity. Structure growth ends once the radiation density comes to dominate again at time t_R , which is defined by $\rho_R(t_R) = \langle \rho_Q(t_R) \rangle$.

PBH production in this mechanism can be analyzed by first calculating the energy density of Q balls at t_f that will eventually form black holes by t_R by weighting the Q -ball energy density M/V by the collapse fraction/probability β evaluated at t_R , and then redshifting this value appropriately. In addition, one must sum the contributions of all length scales V through a coarse-graining procedure. This is accomplished for some arbitrary function $g(V)$ via the procedure

$$\sum_{\{V\}} g(V) = g(V_1) + g(V_1/\chi) + \dots = \sum_{i=1}^{I_{\max}} g(V_1\chi^{1-i}) \quad (5)$$

$$\approx \int_1^{I_{\max}} di g(V_1\chi^{1-i}) = \frac{1}{\ln \chi} \int_{V_{\min}}^{V_1} \frac{dV}{V} g(V), \quad (6)$$

where we have used the Euler-Maclaurin summation approximation, $\chi \sim \mathcal{O}(1-10)$ is a parameter of the coarse-graining, and V_{\min} is the smallest volume scale under

consideration, set by N_{\min} . We henceforth take $\chi = e$ for simplicity.

At t_R , the black hole density is given by

$$\langle \rho_{\text{BH}}(t_R) \rangle = \left(\frac{a_f}{a_R} \right)^3 \sum_{N=1}^{\infty} \int_{V_{\min}}^{V_R} \frac{dV}{V} \int_0^{\infty} dM \left(\beta \frac{M}{V} \right) F_Q, \quad (7)$$

where $V_R = (4\pi/3)t_R^3(t_Q/t_R)^2(t_f/t_Q)^{3/2}$ is the size of the comoving horizon at t_R , evaluated at t_f . The black hole energy density then redshifts like nonrelativistic matter, $\langle \rho_{\text{BH}}(t) \rangle = \langle \rho_{\text{BH}}(t_R) \rangle (a_R/a(t))^3$.

The mass function $d\langle \rho_{\text{BH}} \rangle / dM$ can be evaluated using the integrand of Eq. (7) ($\langle \rho_{\text{BH}} \rangle = \int dM d\langle \rho_{\text{BH}} \rangle / dM$). Using this ‘‘differential density’’ mass function, shown in Fig. 2, one can glean some information regarding how the parameters of the theory affect the distribution of black hole mass. We find that the spectrum depends only on the dimensionless parameters N_f , $\eta = M/M_f$, $r_f = t_Q/t_f$, and $r = t_R/t_Q$ (given this set, plus a value for t_f , fixes the remaining parameters τ_Q , M_f due to consistency conditions on the boundary of the Q -ball dominated era). First, it is obvious from the normalization of each curve that the lower the number of Q balls per horizon, the more black holes are created. This is expected, as the Poisson statistics suppress the density fluctuations for large Q -ball number. Second, there is a hard lower cutoff in the PBH mass, which occurs at $\eta = N_{\min}/N_f$. Above that, the BH number sharply increases with a power law $\propto \eta^{2.7}$; the extent of this region depends on the magnitude of r , with larger values leading to a larger range. Above that, the spectrum becomes approximately flat ($\propto \eta^{-0.15}$), meaning that the number of black holes in each decade of mass is comparable. Of course, the upper end of this range dominates the energy density of the distribution. Then, at around $M = M_Q$, there is a sharp transition and the slope becomes strongly negative ($\propto \eta^{-4.5}$) due to the reduced growth the superhorizon modes are subject to. Then, there is an upper

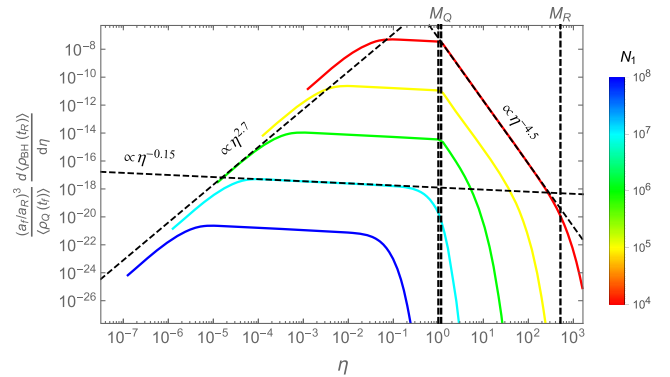


FIG. 2. Differential fraction of Q -ball energy density transferred to BH density as a function of $\eta = M/M_f$. This spectrum corresponds to the parameters for the solid black line in Fig. 3, which accounts for 100% of the dark matter.

exponential cutoff at $\eta \sim 10^8/N_f$ due once again to the Poisson statistics (the cutoff appears to take precedence over previously mentioned transitions). For the parameters given in Fig. 2, the spectrum is highly developed, in the sense that it has been subject to a lengthy matter dominated era of growth ($r \gg 1$).

Experimental constraints can be considered after we evolve the black hole distribution to the present day. In simple terms, we just have to take Eq. (7) and multiply it by $(a(t_0)/a(t_R))^{-3}$. Naïvely, one would use the equation $a_1/a_2 = (t_1/t_2)^n$ (with $n = 1/2$ or $2/3$) keeping in mind that the Universe transitions back to a matter dominated era around $z_{\text{eq}} \approx 3360$. However, an extended Q -ball dominated era ($r \gg 1$) alters the time scale of cosmological thermal history because the radiation temperature is altered by the Q -ball decays and the form of the scale factor during this era. In this case, one must use $a_1/a_2 = g_{*S}^{1/3}(T_2)T_2/g_{*S}^{1/3}(T_1)T_1$ and evolve from T_R [defined by $\rho_R(t_R) = (\pi^2/30)g_*(T_R)T_R^4$] to $T_0 = 2.7 \text{ K} = 2.3 \text{ meV}$. This has the advantage of accurately accounting for any deviation from cosmological history. In addition, we enforce an additional constraint $T_R > T_{\text{BBN}} \sim \text{MeV}$, so that the entropy injection from Q -ball decays does not interfere with nucleosynthesis.

We now apply observational constraints to our model. There are a variety of constraints [9,11,40–43], coming from a number of sources, including gamma rays from Hawking radiation, femto-, micro-, and millilensing, white dwarf capture, pulsar timing arrays, and accretion effects on the cosmic microwave background. These constraints can be observed in Fig. 3 in orange. It is important to note that

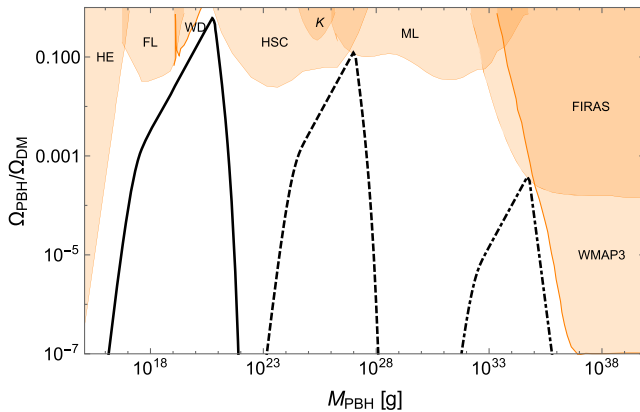


FIG. 3. Comparison of the observational constraints on $f \equiv \Omega_{\text{PBH}}/\Omega_{\text{DM}}$ (orange, shaded), with the expected value of $\tilde{f}_{\text{BH}}(M) \equiv \rho_{\text{DM}}^{-1} d\langle \rho_{\text{BH}} \rangle / d(\ln M)$ for some hand-picked parameters (black). Parameters for the three curves are $t_f = 1.12 \times 10^{-17} \text{ s}$, $r_f = 1.1$, $r = 4.47 \times 10^2$, $N_f = 10^6$, $f = 1$ (solid line), $t_f = 2.0 \times 10^{-11} \text{ s}$, $r_f = 1.1$, $r = 1.58 \times 10^3$, $N_f = 10^6$, $f = 0.2$ (dashed line), and $t_f = 1.0 \times 10^{-3} \text{ s}$, $r_f = 1.1$, $r = 4.47 \times 10^2$, $N_f = 10^5$, $f = 0.001$ (dot-dashed line).

the constraints as plotted only apply for a monochromatic mass distribution. The mass spectrum of this model clearly extends over several decades, and so we must translate these constraints into something applicable to our model. We adopt the procedure outlined in [9], which amounts to comparing the expected dark matter fraction to the constraints on an interval-by-interval basis. As a guide, we also plot $\tilde{f}_{\text{BH}}(M) \equiv \rho_{\text{DM}}^{-1} d\langle \rho_{\text{BH}} \rangle / d(\ln M)$, which gives an approximate idea of how the expected BH density in each logarithmic interval of mass compares with the constraints. We have verified for the given parameters that the constraints have not been violated. We note that the solid curve corresponds to a distribution that makes up 100% of the dark matter with peak black hole mass 10^{20} g . For the case of supersymmetric Q balls with the SUSY-breaking scale $\Lambda_{\text{SUSY}} > 10 \text{ TeV}$, the fragmentation time cannot be much longer than the Hubble time $H^{-1} \sim M_p/g_*^{1/2} \Lambda_{\text{SUSY}}^2 \lesssim 8 \times 10^{-15} \text{ s}$, which corresponds to peak PBH masses of about 10^{23} g . The case illustrated in Fig. 3 satisfies this bound; thus, primordial black holes from supersymmetric Q balls can account for 100% of the dark matter.

The dot-dashed curve corresponds to a distribution that only makes up 0.1% of the dark matter, but has a peak BH mass of $30 M_{\odot}$. This is suggestive, as even if the dark matter is not entirely PBHs, they might still be responsible for some of the black hole merger events detected by LIGO [13].

Topological defect formation can also lead to the production of PBHs if the topological defects come to dominate the energy density. The analysis is sufficiently different from that of Q balls, primarily because typically only one defect per horizon is produced at the time of formation due to the Kibble mechanism [44]. However, the general mechanism remains the same: small number densities of defects lead to large fluctuations relative to the background density, these fluctuations become gravitationally bound and collapse to form black holes once the relic density has come to dominate, and the relics decay due to some instability (such as gravitational waves or decay to Nambu-Goldstone bosons in the case of cosmic strings). In order to accurately model production of PBHs from these defects, one should calculate the expected density perturbations on initially superhorizon scales, which only begin to grow once these scales pass back within the horizon and the defects come to dominate the Universe's energy density. Cosmic strings are probably the most likely candidate for primordial relics due to the fact that they are typically cosmologically safe, as the energy density in string loops is diluted during expansion at the same rate as radiation, a^{-4} [45,46].

We have shown that number density fluctuations of nontopological solitons in the early Universe can be responsible for production of primordial black holes, and furthermore, that these black holes can make up all or part of the dark matter. Scalar fields and Q -ball formation are

generic features of supersymmetric extensions of the standard model, which provides a good motivation for this mechanism. Other scalar fields may exist and may undergo fragmentation, leading to PBH formation. In addition, we have elucidated a possible mechanism through which topological defects may be able to produce primordial black holes as well under certain circumstances.

This work was supported by the U.S. Department of Energy Award No. DE-SC0009937. A. K. was also supported by the World Premier International Research Center Initiative (WPI), MEXT, Japan.

-
- [1] Y. B. Zel'dovich and I. D. Novikov, *Sov. Astron.* **10**, 602 (1967).
- [2] S. Hawking, *Mon. Not. R. Astron. Soc.* **152**, 75 (1971).
- [3] B. J. Carr and S. W. Hawking, *Mon. Not. R. Astron. Soc.* **168**, 399 (1974).
- [4] J. Garcia-Bellido, A. D. Linde, and D. Wands, *Phys. Rev. D* **54**, 6040 (1996).
- [5] M. Yu. Khlopov, *Res. Astron. Astrophys.* **10**, 495 (2010).
- [6] P. H. Frampton, M. Kawasaki, F. Takahashi, and T. T. Yanagida, *J. Cosmol. Astropart. Phys.* 04 (2010) 023.
- [7] M. Kawasaki, A. Kusenko, and T. T. Yanagida, *Phys. Lett. B* **711**, 1 (2012).
- [8] M. Kawasaki, A. Kusenko, Y. Tada, and T. T. Yanagida, *Phys. Rev. D* **94**, 083523 (2016).
- [9] B. Carr, F. Kuhnel, and M. Sandstad, *Phys. Rev. D* **94**, 083504 (2016).
- [10] K. Inomata, M. Kawasaki, K. Mukaida, Y. Tada, and T. T. Yanagida, *Phys. Rev. D* **95**, 123510 (2017).
- [11] K. Inomata, M. Kawasaki, K. Mukaida, Y. Tada, and T. T. Yanagida, [arXiv:1701.02544](https://arxiv.org/abs/1701.02544).
- [12] J. Georg and S. Watson, [arXiv:1703.04825](https://arxiv.org/abs/1703.04825).
- [13] S. Bird, I. Cholis, J. B. Muñoz, Y. Ali-Haïmoud, M. Kamionkowski, E. D. Kovetz, A. Raccanelli, and A. G. Riess, *Phys. Rev. Lett.* **116**, 201301 (2016).
- [14] T. Nakamura, M. Sasaki, T. Tanaka, and K. S. Thorne, *Astrophys. J.* **487**, L139 (1997).
- [15] S. Clesse and J. García-Bellido, *Phys. Rev. D* **92**, 023524 (2015).
- [16] T. S. Bunch and P. C. W. Davies, *Proc. R. Soc. A* **360**, 117 (1978).
- [17] A. D. Linde, *Phys. Lett.* **116B**, 335 (1982).
- [18] I. Affleck and M. Dine, *Nucl. Phys.* **B249**, 361 (1985).
- [19] A. A. Starobinsky and J. Yokoyama, *Phys. Rev. D* **50**, 6357 (1994).
- [20] A. Kusenko and M. E. Shaposhnikov, *Phys. Lett. B* **418**, 46 (1998).
- [21] M. Dine and A. Kusenko, *Rev. Mod. Phys.* **76**, 1 (2003).
- [22] S. R. Coleman, *Nucl. Phys.* **B262**, 263 (1985); **269**, 744(E) (1986).
- [23] A. Kusenko, *Phys. Lett. B* **405**, 108 (1997).
- [24] A. Kusenko, *Phys. Lett. B* **404**, 285 (1997).
- [25] G. R. Dvali, A. Kusenko, and M. E. Shaposhnikov, *Phys. Lett. B* **417**, 99 (1998).
- [26] K. Enqvist and J. McDonald, *Phys. Lett. B* **425**, 309 (1998).
- [27] K. Enqvist and J. McDonald, *Nucl. Phys.* **B538**, 321 (1999).
- [28] S. Kasuya and M. Kawasaki, *Phys. Rev. D* **61**, 041301 (2000).
- [29] S. Kasuya and M. Kawasaki, *Phys. Rev. D* **62**, 023512 (2000).
- [30] A. G. Cohen, S. R. Coleman, H. Georgi, and A. Manohar, *Nucl. Phys.* **B272**, 301 (1986).
- [31] M. Kawasaki and M. Yamada, *Phys. Rev. D* **87**, 023517 (2013).
- [32] K. Enqvist and J. McDonald, *Phys. Lett. B* **440**, 59 (1998).
- [33] A. Kusenko, L. C. Loveridge, and M. Shaposhnikov, *J. Cosmol. Astropart. Phys.* 08 (2005) 011.
- [34] M. Kawasaki, K. Konya, and F. Takahashi, *Phys. Lett. B* **619**, 233 (2005).
- [35] S. Kasuya and M. Kawasaki, *Phys. Rev. D* **89**, 103534 (2014).
- [36] E. Cotner and A. Kusenko, *Phys. Rev. D* **94**, 123006 (2016).
- [37] R. J. Scherrer and M. S. Turner, *Phys. Rev. D* **31**, 681 (1985).
- [38] A. G. Polnarev and M. Yu. Khlopov, *Usp. Fiz. Nauk* **145**, 369 (1985) [*Sov. Phys. Usp.* **28**, 213 (1985)].
- [39] J. Georg, G. Şengör, and S. Watson, *Phys. Rev. D* **93**, 123523 (2016).
- [40] B. J. Carr, K. Kohri, Y. Sendouda, and J. Yokoyama, *Phys. Rev. D* **81**, 104019 (2010).
- [41] F. Kuhnel and K. Freese, *Phys. Rev. D* **95**, 083508 (2017).
- [42] H. Niikura, M. Takada, N. Yasuda, R. H. Lupton, T. Sumi, S. More, A. More, M. Oguri, and M. Chiba, [arXiv:1701.02151](https://arxiv.org/abs/1701.02151).
- [43] Y. Inoue and A. Kusenko, [arXiv:1705.00791](https://arxiv.org/abs/1705.00791)
- [44] T. W. B. Kibble, *J. Phys. A* **9**, 1387 (1976).
- [45] T. Vachaspati and A. Vilenkin, *Phys. Rev. D* **30**, 2036 (1984).
- [46] N. Turok, *Phys. Lett.* **123B**, 387 (1983).